IBEHS 4A03 Assignment #2
Baoze Lin, Hady Ibrahim

---

1. Question 1

(1.1) The pole-zero maps for $Y_1(s)$ and $Y_2(s)$ help us see system stability.
- The left plot shows the pole-zero locations for $Y_1(s)$, which has poles in the left half-plane, indicating a stable system (converging). It is not oscillatory since there are no imaginary parts to the poles. The poles are: $s = 0, -2, -3$.
- The right plot for $Y_2(s)$ shows at minimum 1 pole in the right half-plane, meaning the system is unstable and will have an exponentially growing response (diverging). It is oscillatory since there are imaginary parts to the poles. The poles are: $s = 0, 2, 1 + 2i, 1 - 2i$.

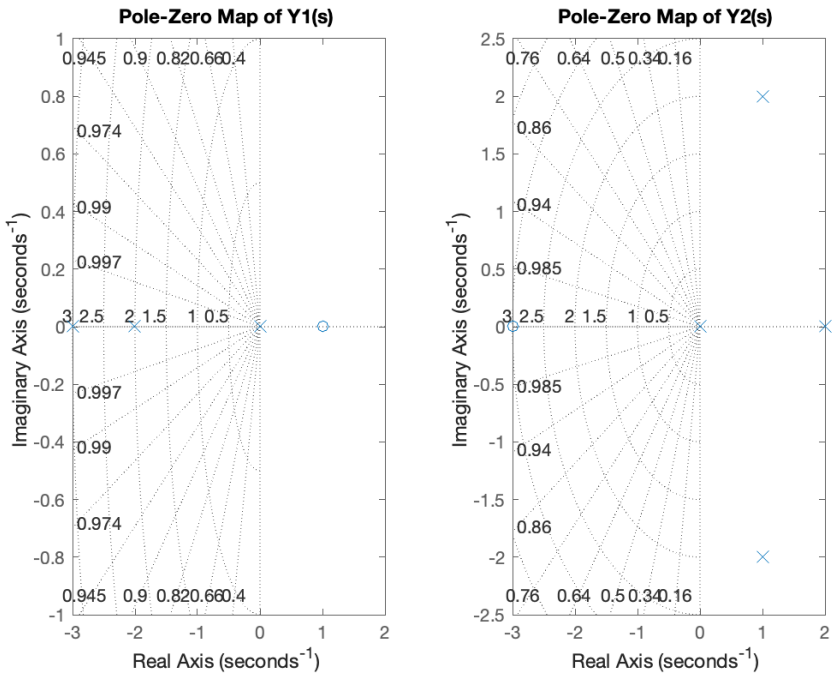

Figure 1: Pole-Zero Maps for $Y_1(s)$ and $Y_2(s)$

(1.2) The Final Value Theorem was used to determine the steady-state values (via hand calculation and using limit() in Matlab):

$$\lim_{t\to\infty} y_1(t) = \lim_{s\to 0} sY_1(s) = -\frac{1}{6}$$

$$\lim_{t\to\infty} y_2(t) = \lim_{s\to 0} sY_2(s) = -\frac{3}{10}$$

Q1

b) $\lim_{t\to\infty} y_1(t) = \lim_{s\to 0} sY_1(s) = \dfrac{s(s-1)e^{-s}}{s(s+2)(s+3)}$

$= \dfrac{-1}{6}$

$\lim_{t\to\infty} y_2(t) = \lim_{s\to 0} sY_2(s) = \dfrac{s(s+3)}{s(s-2)(s^2-2s+5)}$

$= \dfrac{3}{(-2)(5)}$

$= \dfrac{-3}{10}$

Figure 2: Final Value Theorem for $Y_1(s)$ and $Y_2(s)$

The calculations confirm that $Y_1(s)$ settles to a finite negative value, whereas $Y_2(s)$ is a diverging system so FVT does not apply in this case. The final value does not exist for $Y_2(s)$. We calculated the FVT anyway just to show that it will not always come up with infinity and you must know the system's stability.

(1.3) The impulse response for both systems was computed to observe the effect of the pole locations.

- The response of $Y_1(s)$ looks to be bounded confirming stability.
- The response of $Y_2(s)$ grows exponentially, which aligns with its unstable pole.

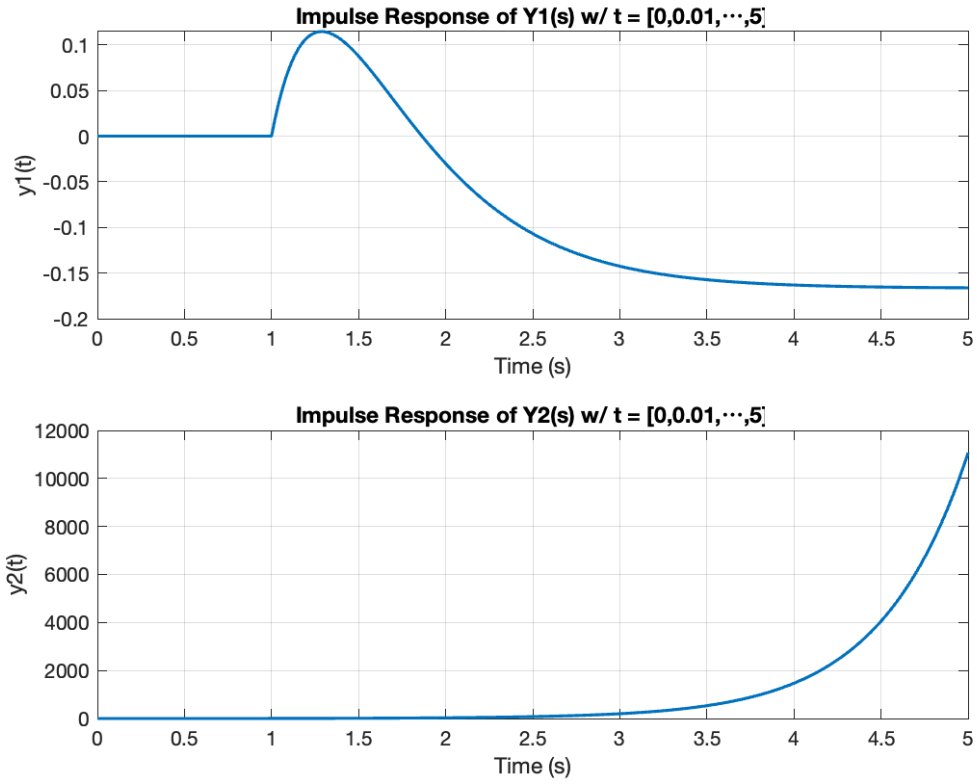

Figure 3: Impulse Response of $Y_1(s)$ and $Y_2(s)$ for $t \in [0, 5]$

Extending the time range further highlights the unstable growth of $Y_2(s)$. Not only that, if you zoom into $Y_1(s)$, you can see that the curve looks a little patchy since the time steps aren't small enough:

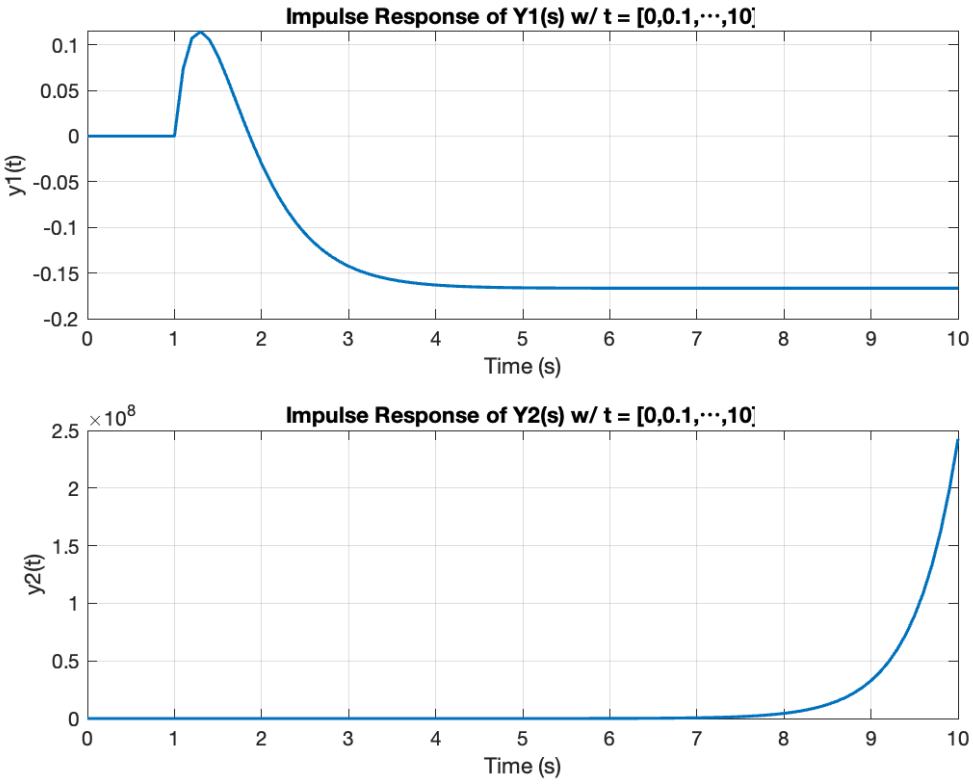

Figure 4: Impulse Response of $Y_1(s)$ and $Y_2(s)$ for $t \in [0, 10]$

2. Question 2

(2.1) Below we've derived the transfer function model that relates the change in temperature of the thermocoupled T to a change in the furnace temperature T_F.

2.1 $\frac{dT}{dt} = \frac{\epsilon A \sigma}{mc_p}(T_F^4 - T^4)$ } $f(t)$

$\left.\frac{\partial f}{\partial T_F}\right|_{\bar{T}_F, \bar{T}} = \frac{4\epsilon A\sigma}{mc_p}\bar{T}_F^3 \qquad \left.\frac{\partial f}{\partial T}\right|_{\bar{T}_F, \bar{T}} = -\frac{4\epsilon A\sigma}{mc_p}\bar{T}^3$

$\frac{dT'}{dt} = \frac{4\epsilon A\sigma}{mc_p}\bar{T}_F^3 \cdot T_F' - \frac{4\epsilon A\sigma}{mc_p}\bar{T}^3 \cdot T'$

$= \frac{4\epsilon A\sigma}{mc_p}\bar{T}^3(T_F' - T')$

Laplace! $sT'(s) = \frac{4\epsilon A\sigma}{mc_p}\bar{T}_F^3 T_F'(s) - \frac{4\epsilon A\sigma}{mc_p}\bar{T}^3 T'(s)$

$T'(s)\left[s + \frac{4\epsilon A\sigma}{mc_p}\bar{T}^3\right] = \frac{4\epsilon A\sigma}{mc_p}\bar{T}_F^3 T_F'(s)$

$\frac{T'(s)}{T_F'(s)} = \frac{\frac{4\epsilon A\sigma}{mc_p}\bar{T}_F^3}{s + \frac{4\epsilon A\sigma}{mc_p}\bar{T}^3}$

$= \frac{\bar{T}_F^3}{\frac{mc_p}{4\epsilon A\sigma}s + \bar{T}^3}$

Figure 5: Hand calculation to find $T'(s)/T_F'(s)$

(2.2) The thermocouple's response to a 30°C drop in furnace temperature was simulated using the linearized transfer function. The step response of the thermocou-

ple shows a gradual decrease in temperature, confirming that the thermocouple lags behind furnace temperature changes. The temperature after 10 seconds was 1360.57 K.

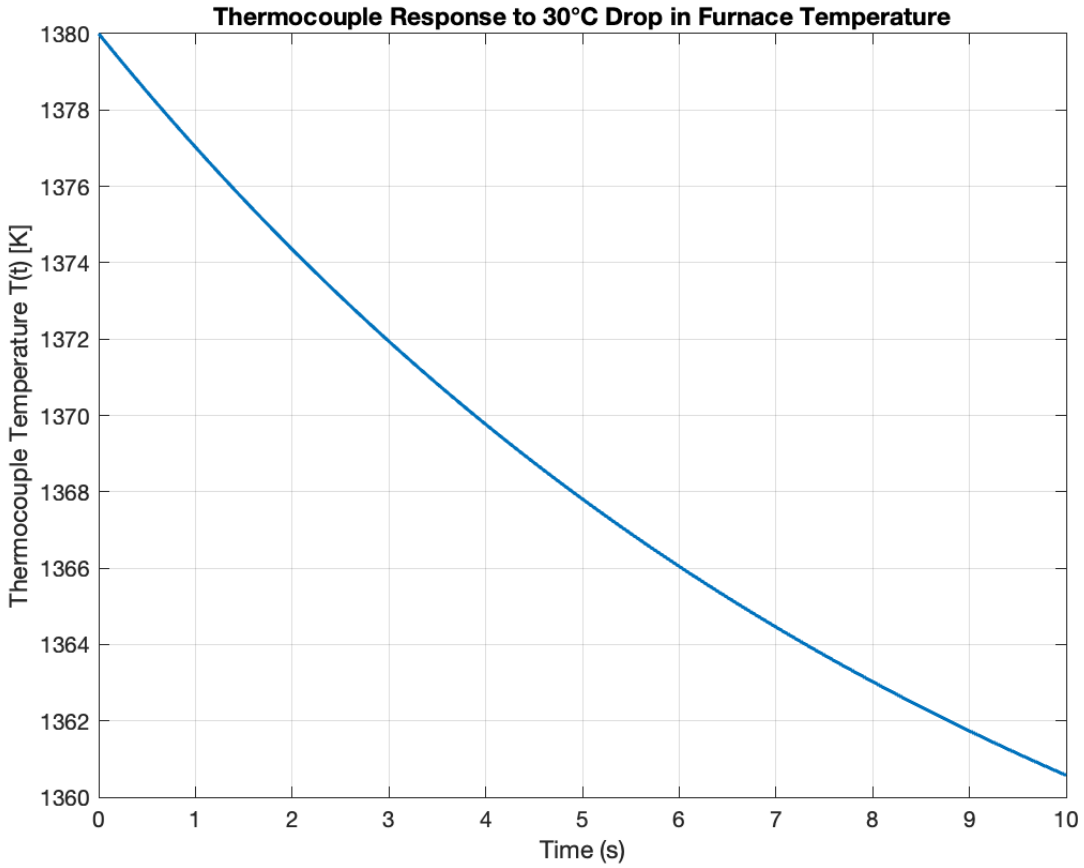

Figure 6: Thermocouple Response to 30°C Drop in Furnace Temperature

(2.3) The nonlinear ODE model for the thermocouple temperature was simulated using ode45(). The resulting response follows a slightly curved trajectory, showing a more gradual cooling effect compared to the linearized model. You can see here, that it is very similar to the linearized model, it is a little more rapid towards the start and then slows down as time goes on. The temperature after 10 seconds was 1361.07 K.

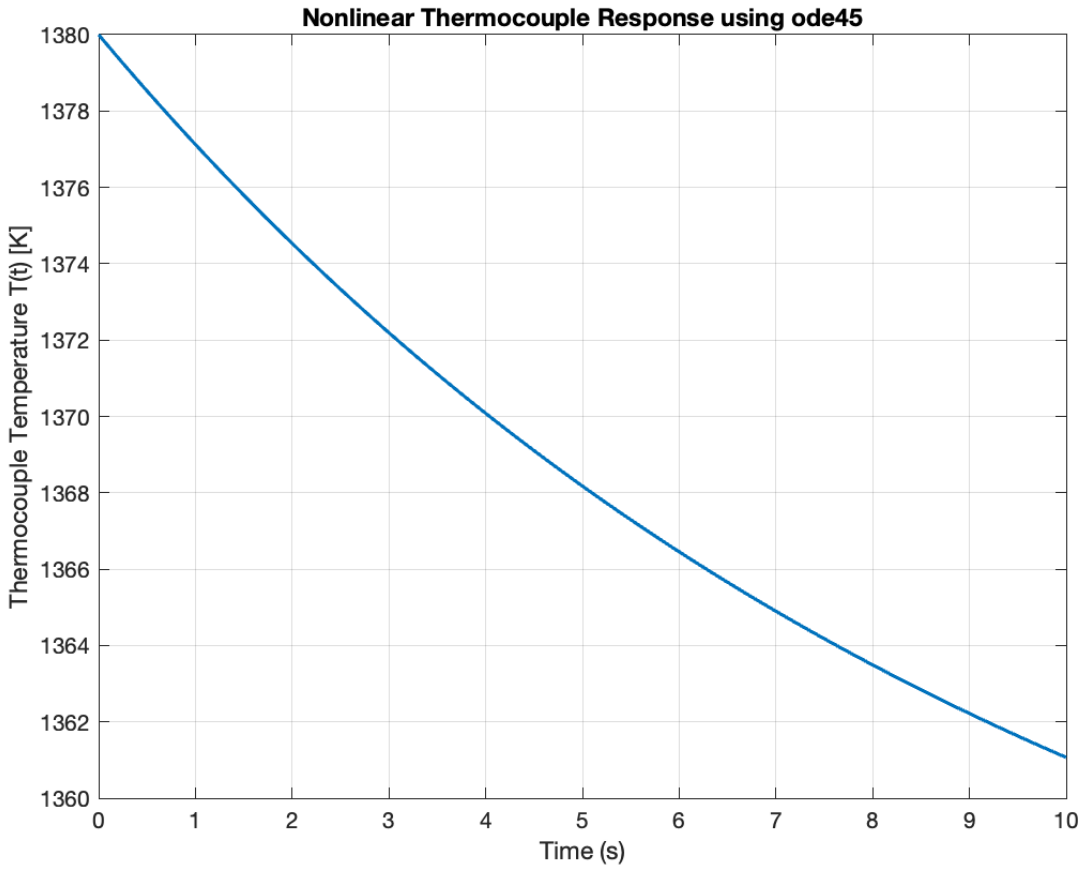

Figure 7: Nonlinear Thermocouple Response using ode45

(2.4) Radiative heat transfer follows the Stefan-Boltzmann Law, which is temperature-dependent and nonlinear. This means the rate of heat loss changes more significantly at higher temperatures compared to a simple linear approximation. Due to this, we expected to see that a comparison of the linear and nonlinear models would show that the linearized transfer function underestimates the cooling rate. What we actually saw was that with a -30°C change in temperature, the linearized model predicts a faster response by just a little compared to the nonlinear model. With the +30°C change, the non-linear model was a little faster, but again very similar responses. This shows that the linearized model estimated

the true temperature quite well.

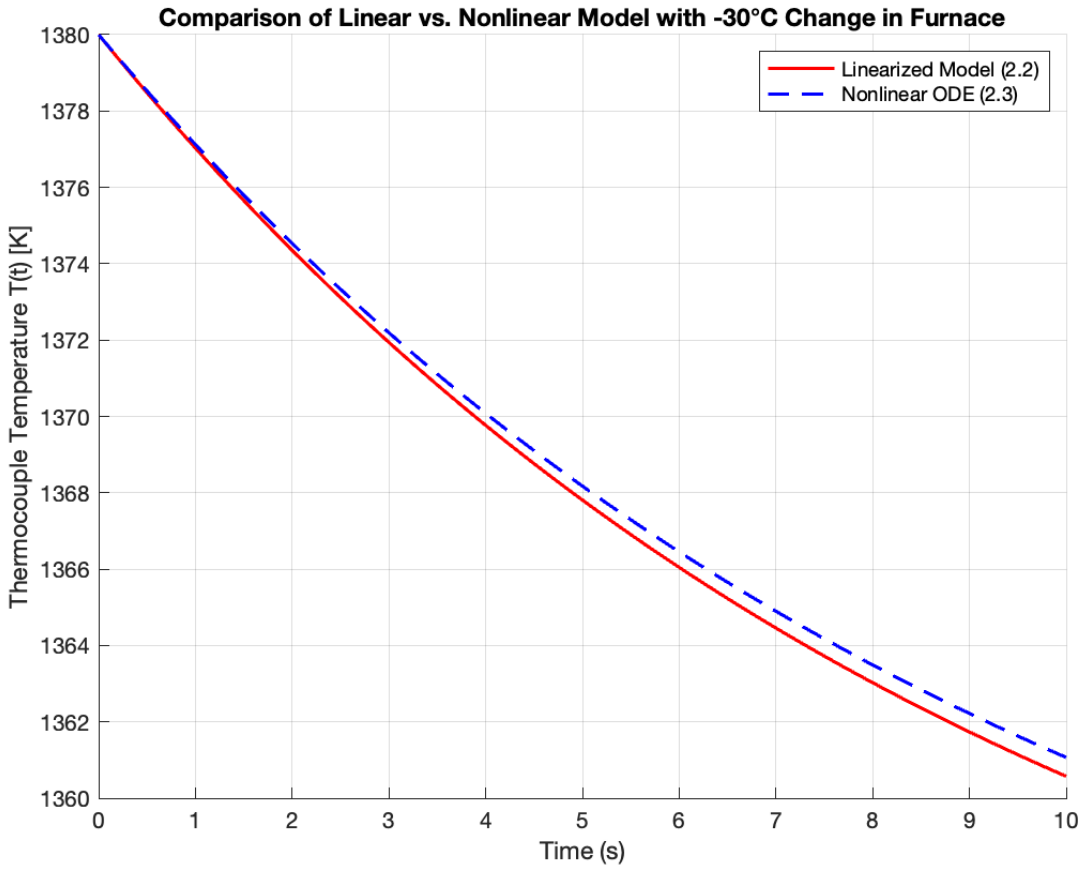

Figure 8: Comparison of Linear vs. Nonlinear Model with +30°C Change in Furnace

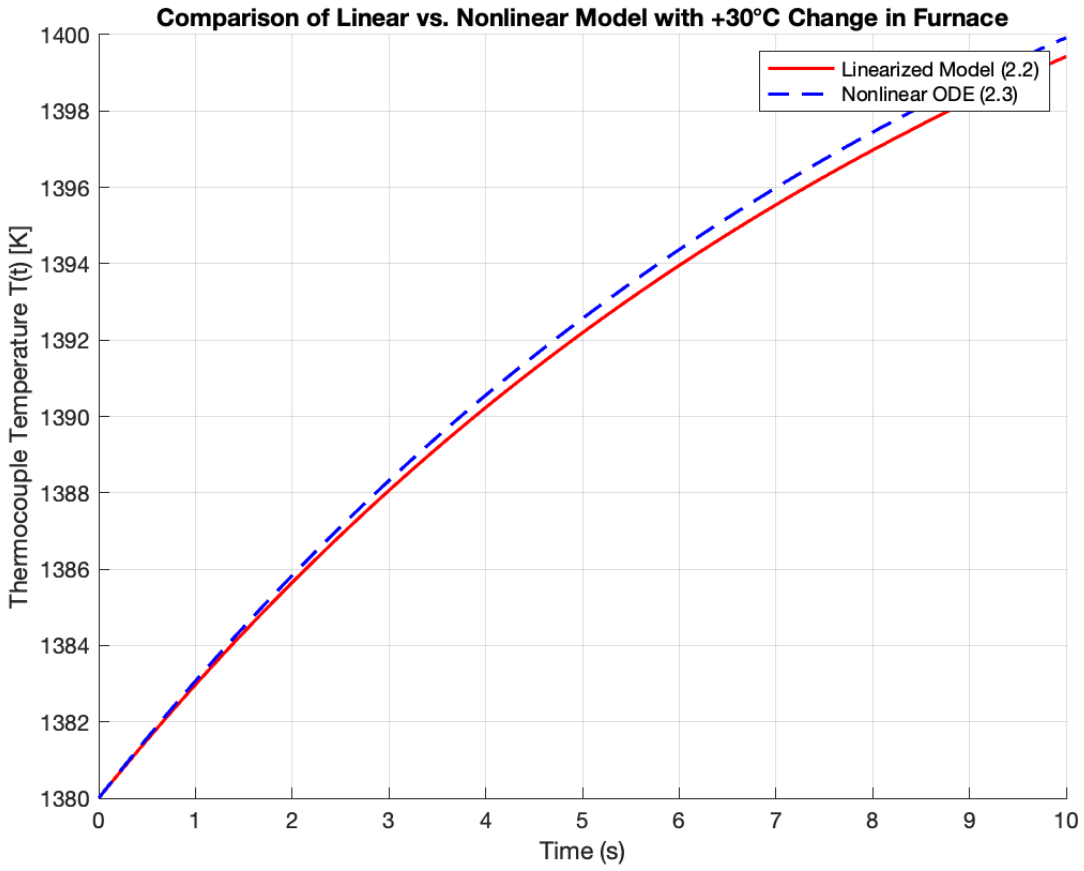

Figure 9: Comparison of Linear vs. Nonlinear Model with -30°C Change in Furnace

(2.5) In this case, we analyzed the effect of heat input $Q(t)$ on the thermocouple temperature. The furnace response to $Q(t)$ was modeled, and the thermocouple's response was calculated by multiplying the transfer functions:

$$\frac{T(s)}{Q(s)} = \frac{T(s)}{T_F(s)} \times \frac{T_F(s)}{Q(s)}$$

The results show that the furnace temperature $T_F(t)$ increases rapidly in response to the applied heat input and reaches its steady-state value within a few seconds.

In contrast, the thermocouple temperature $T(t)$ rises much more gradually indicating a significant time delay in its response.

This delay occurs because the thermocouple absorbs heat primarily through radiation, which is a slower process compared to the direct heating of the furnace. As a result, the thermocouple reading does not immediately reflect the actual furnace temperature, but instead lags behind, converging toward the final temperature over time (which it doesn't even reach in the 10 seconds).

In control applications, this measurement lag is critical to know because relying solely on $T(t)$ for feedback could lead to delayed or incorrect adjustments. To improve performance, a control system should account for this delay and maybe add some other elements or logic to work around it.

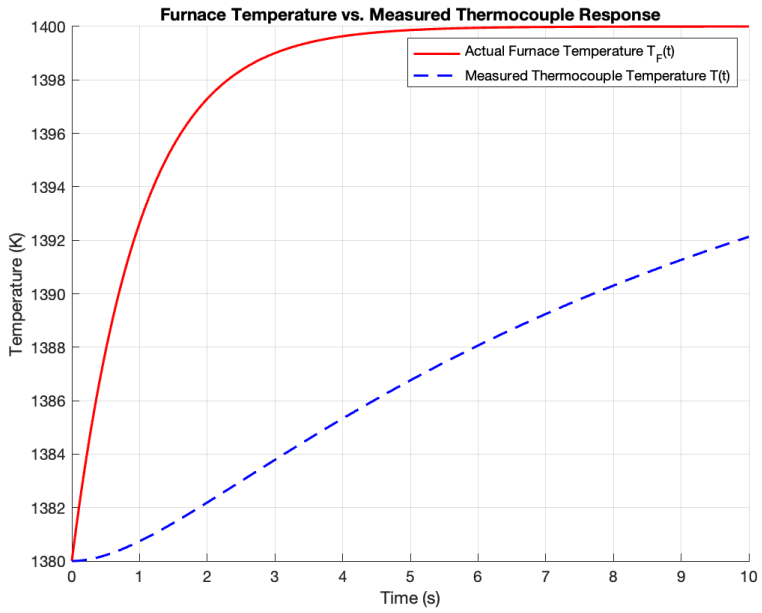

Figure 10: Furnace Temperature vs. Measured Thermocouple Response with Heat Input Q

3. Question 3

(3.1) The given transfer function is:

$$\frac{V(s)}{P(s)} = \frac{AK_{P\to V}}{\rho ALs^2 + bs + c}$$

To rewrite it in standard form, divide the numerator and denominator by c to isolate the 1 in the denominator:

$$\frac{V(s)}{P(s)} = \frac{\frac{AK_{P\to V}}{c}}{\frac{\rho AL}{c}s^2 + \frac{b}{c}s + 1}$$

We define the following from the standard form of a second order transfer function:

$$K = \frac{AK_{P\to V}}{c}, \quad \tau^2 = \frac{\rho AL}{c}, \quad 2\zeta\tau = \frac{b}{c}$$

The transfer function in standard form becomes the below with the above definitions:

$$\frac{V(s)}{P(s)} = \frac{K}{\tau^2 s^2 + 2\zeta\tau s + 1}$$

(3.2) The process gain K relates the steady-state change in the output voltage ($V(t)$) to the steady-state change in the input pressure ($P(t)$). From both the step test diagram given in the assignment and also Empirical_Data.csv, we observe a steady-state output voltage of around 20 mV when the input pressure step test is 2 units. Since the process gain K is defined as:

$$K = \frac{\Delta V}{\Delta P}$$

Substituting the given values:

$$K = \frac{20}{2} = 10$$

Thus, the process gain for this system is $K = 10$.

(3.3) Using the Matlab code presented in Problem3.m, we can estimate the time constant τ and damping ratio ζ of the system using the approach described by the question – a double for loop and a sum-of-squared-errors calculation. The code iterates through various values of τ and ζ to find the pair that minimizes the sum-of-squared-errors between the step test data and the transfer function model.

The optimized values are 0.61 for tau and 0.33 for zeta. They occur with a minimal sum-of-squared-errors of 43.0861. The quality of the fit is demonstrated below.

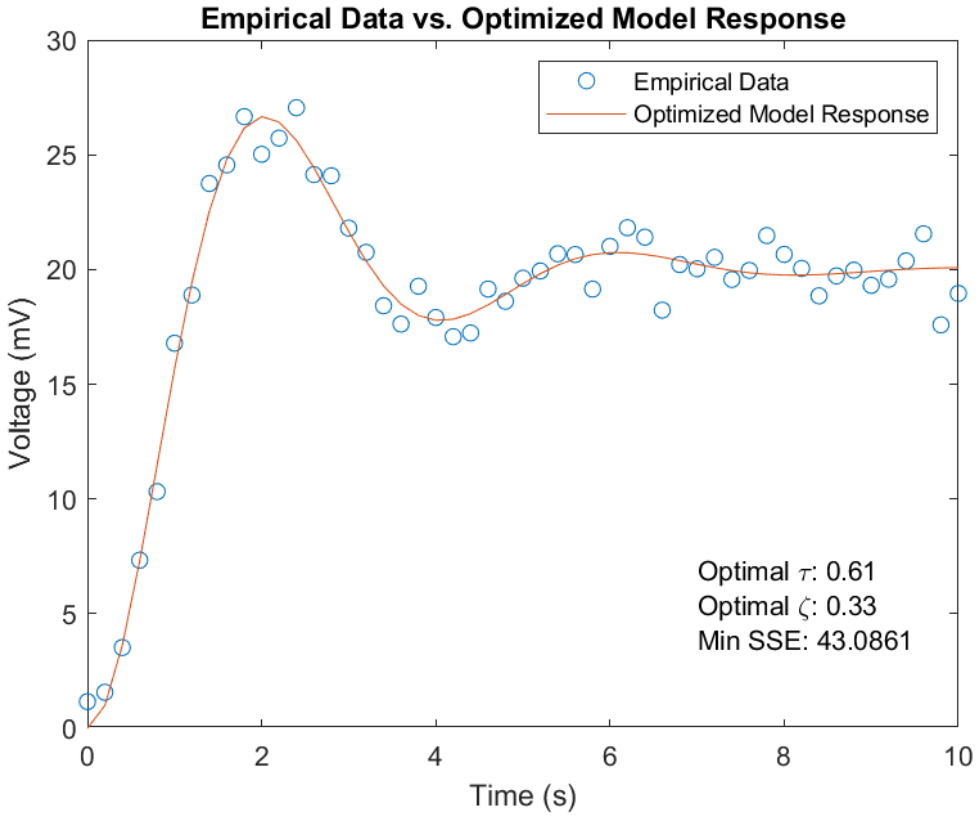

Figure 11: Fitting the Transfer Function to the Step Test Data

(3.4) Based on the above determination of the optimized values for tau and zeta as well as the formulas for the variables we determined earlier, we obtain the following values:

i. $c \triangleq$ lineal friction of the fluid moving through the catheter:

$$c = \frac{\rho A L}{\tau^2}$$

Substituting the given values:

$$\rho = 0.62, \quad A = 0.20, \quad L = 6, \quad \tau = 0.61$$

$$c = \frac{0.62 \cdot 0.20 \cdot 6}{(0.61)^2} = \frac{0.744}{0.3721} = 1.9995 \approx 2.00$$

ii. $b \triangleq$ viscous friction of the fluid in moving through the catheter:

$$b = 2\zeta\tau c$$

Substituting the values:

$$\zeta = 0.33, \quad \tau = 0.61, \quad c = 2.00$$

$$b = 2 \cdot 0.33 \cdot 0.61 \cdot 2.00 = 0.8050 \approx 0.81$$

iii. $K_{P\to V} \triangleq$ gain that relates a change in output voltage to a change in pressure: From the process gain K, we know:

$$K = \frac{A K_{P\to V}}{c}$$

Rearranging for $K_{P\to V}$:

$$K_{P\to V} = \frac{Kc}{A}$$

Substituting the values:

$$K = 10, \quad c = 2.00, \quad A = 0.20$$

$$K_{P\to V} = \frac{10 \cdot 2.00}{0.20} = \frac{20}{0.20} = 99.9731 \approx 100$$

Therefore, the approximated final values are:

$$c = 2.00, \quad b = 0.81, \quad K_{P\to V} = 100$$

4. Question 4

(4.1) The linearized equations and the derivation is shown below:

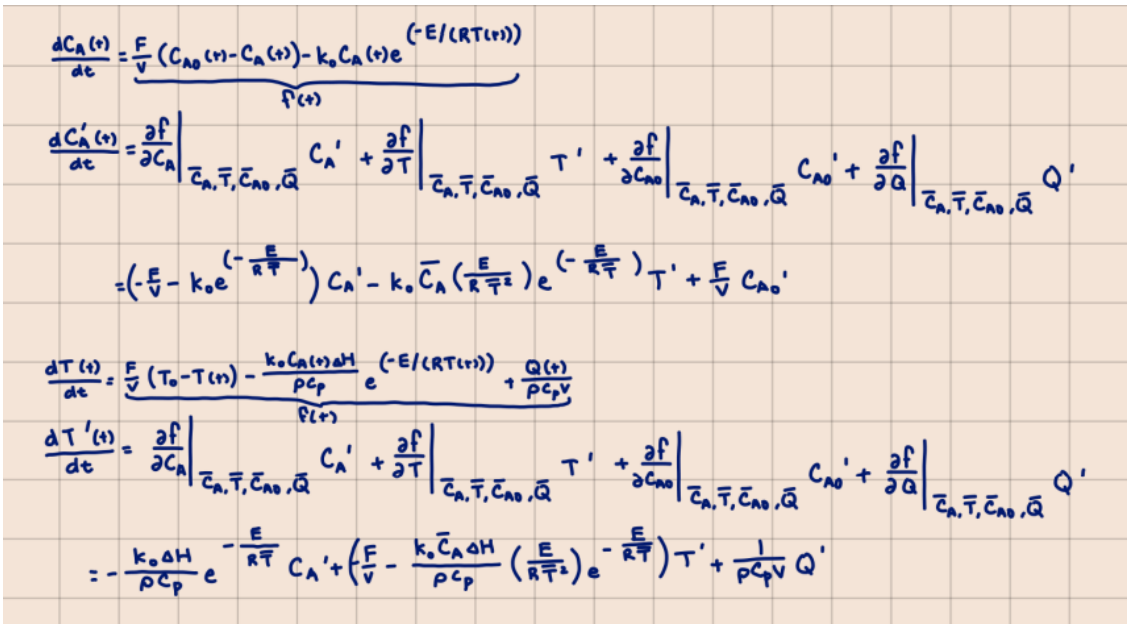

Figure 12: Linearized Equations for the Non-Isothermal Stirred Tank Bioreactor

The linearized equations in deviation form are:

i. Linearized Material Balance:

$$\frac{dC_A'(t)}{dt} = \left(-\frac{F}{V} - k_0 e^{-\frac{E}{RT}}\right) C_A'(t) - k_0 \bar{C}_A \frac{E}{R\bar{T}^2} e^{-\frac{E}{RT}} T'(t) + \frac{F}{V} C_{A0}'(t).$$

ii. Linearized Energy Balance:

$$\frac{dT'(t)}{dt} = -\frac{k_0 \Delta H}{\rho c_p} e^{-\frac{E}{RT}} C_A'(t) + \left(-\frac{F}{V} - \frac{k_0 \bar{C}_A \Delta H}{\rho c_p} e^{-\frac{E}{RT}} \frac{E}{R\bar{T}^2}\right) T'(t) + \frac{Q'(t)}{\rho c_p V}.$$

(4.2) Using the original non-linearized equations and the fact that the system is at steady state, We have the math below:

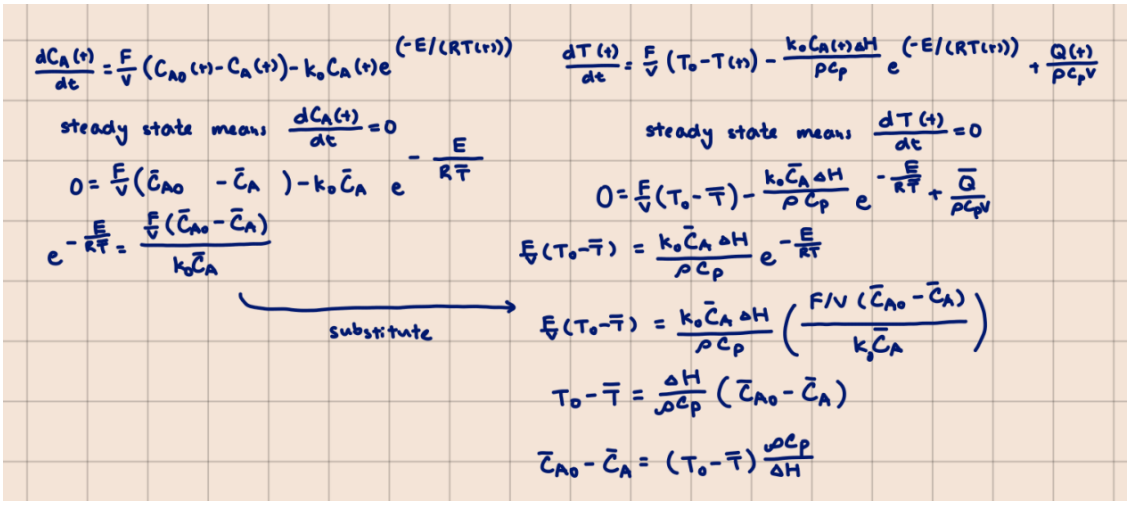

Figure 13: Nonlinear Steady-State Equations for the Non-Isothermal Stirred Tank Bioreactor

We now obtain the below equations that describe the system:

$$e^{-\frac{E}{RT}} = \frac{\frac{F}{V}(\bar{C}_{A0} - \bar{C}_A)}{k_0 \bar{C}_A}$$

$$\bar{C}_{A0} - \bar{C}_A = (T_0 - \bar{T})\frac{\rho C_p}{\Delta H}$$

This system can be solved in Matlab using the fsolve() function, as done in the code presented in Problem4.m. There are several equilibria for this problem, so we need to provide an initial guess for the solver to converge to the correct solution. The initial guess will be a value really close to the provided equilibrium value in the question, $\bar{C}_A = 0.0199$ kmol $\cdot$ m^{-3}, $\bar{T} = 448.09$ K. We use 0.02 and 449 as the initial guesses for the solver. The optimized values as determined by the solver is shown below.

```
Steady-state CA_bar = 0.0199 kmol/m^3
Steady-state T_bar = 448.09 K
```

Figure 14: Optimized Equilibrium Values for the Nonlinear Non-Isothermal Stirred Tank Bioreactor

(4.3) The linearized and nonlinearized models were simulated in Matlab to compare

their responses. We expect the linearized model to be a good approximation for small deviations from the equilibrium point.

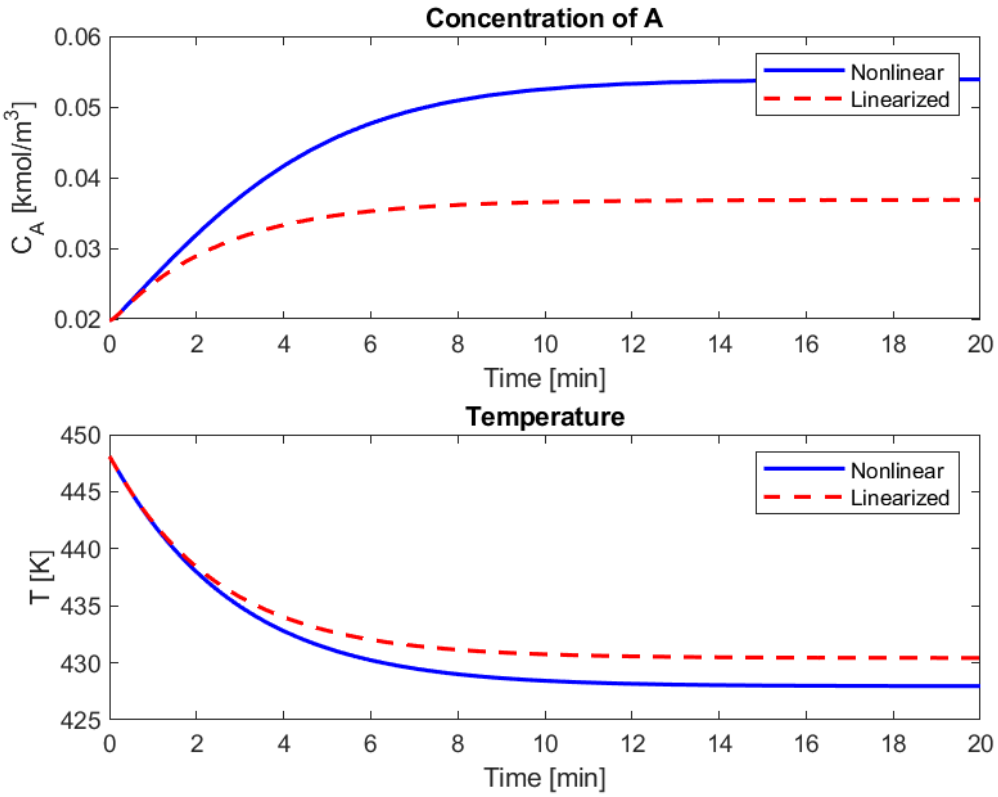

Figure 15: Comparison of Linearized and Nonlinearized Pendulum Models

The linearized model is accurate for small deviations from the steady state. However, for larger deviations, the linearized model becomes less accurate, particularly for the concentration of C_A, as the nonlinear effects of the reaction rate ($k_0 C_A e^{-\frac{E}{RT}}$) become significant. The nonlinear system captures the full reaction, while the linearized system approximates these dynamics but cannot fully capture the nonlinear interactions between C_A and T. The linearized model is useful for control system design and small perturbations around the steady state, where it provides a good approximation of the system dynamics. However, for larger perturbations, such as significant cooling or heating, the nonlinear model should be used to ensure accurate predictions.

(4.4) The transfer functions are derived in the following figures. We firstly can derive the transfer functions $\frac{C'_A(s)}{C'_{A0}(s)}$ and $\frac{T'(s)}{Q'(s)}$. Since the Laplace of the linearized equation contains the inputs C'_{A0} and Q', we can derive the transfer functions by isolating the Laplace of the output. We can omit the other input as we are isolating a transfer function.

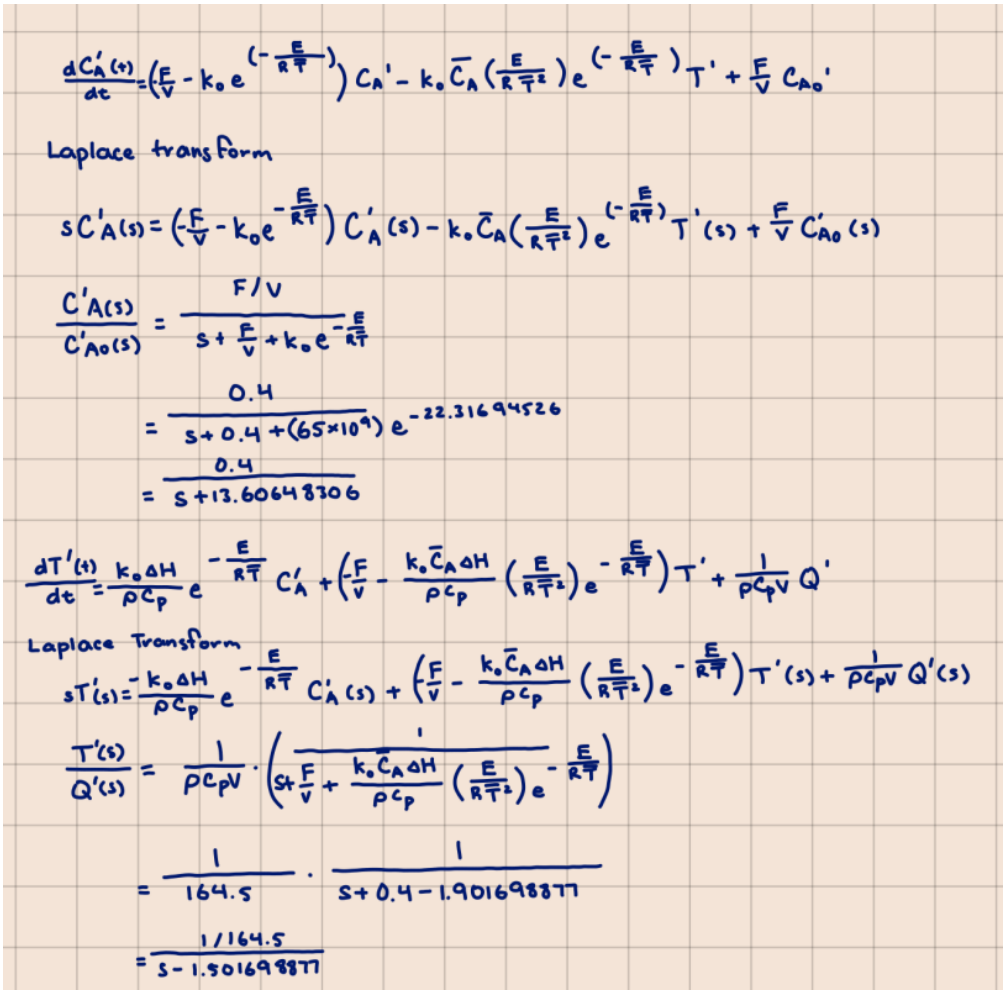

Figure 16: Transfer Functions $\frac{C'_A(s)}{C'_{A0}(s)}$ and $\frac{T'(s)}{Q'(s)}$

The next transfer functions are more complicated as the inputs don't exist in the linearized equation for the output. In order to see the effect of the input on the output variable for transfer functions $\frac{C'_A(s)}{Q'(s)}$ and $\frac{T'(s)}{C'_{A0}(s)}$, we must isolate the

equations for $C'_A(s)$ and $T'(s)$, and then substitute them into the other. We also simplify the constants into variables for easier calculation and legibility.

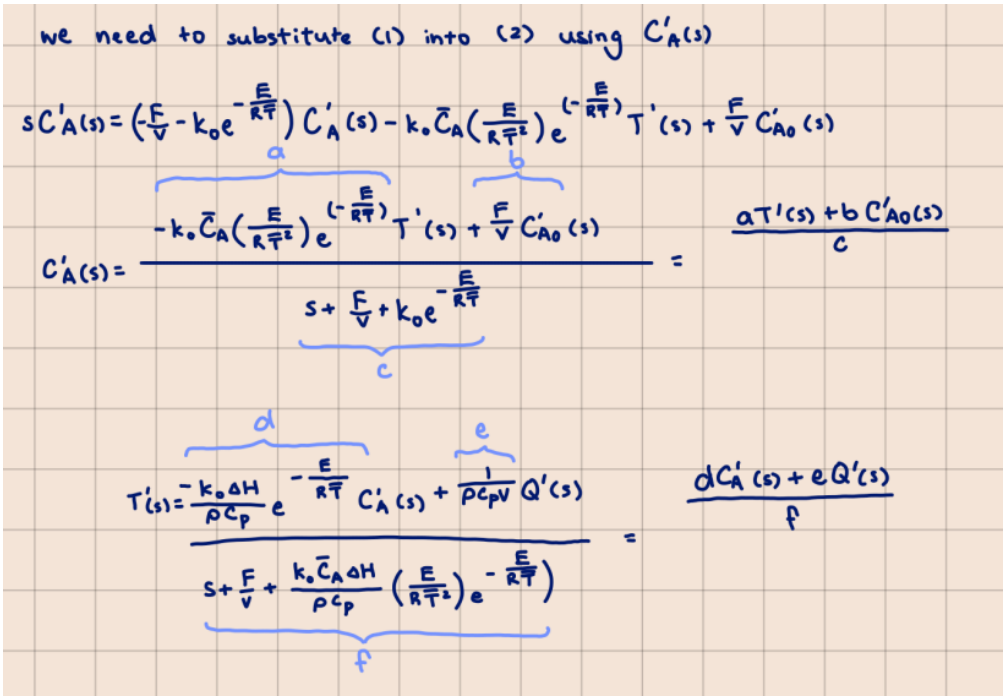

Figure 17: Deriving Transfer Functions $\frac{C'_A(s)}{Q'(s)}$ and $\frac{T'(s)}{C'_{A0}(s)}$ Part 1

Substituting the equations for $C'_A(s)$ and $T'(s)$ into the other, we can derive the transfer functions $\frac{C'_A(s)}{Q'(s)}$ and $\frac{T'(s)}{C'_{A0}(s)}$.

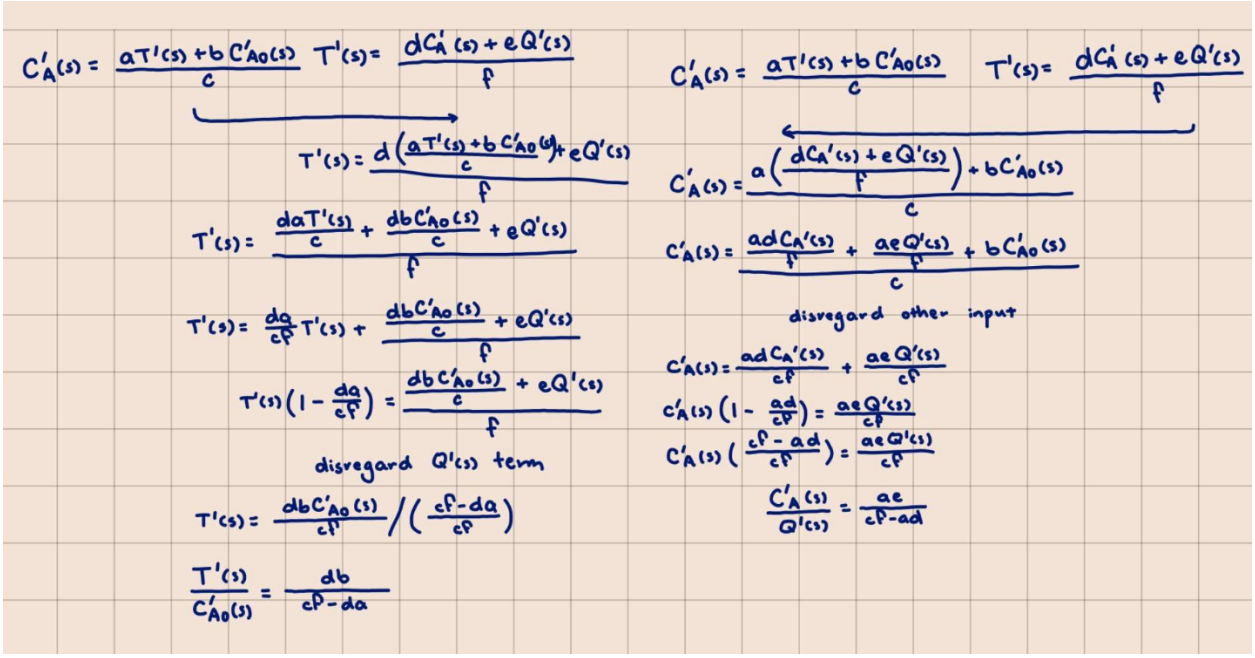

Figure 18: Deriving Transfer Functions $\frac{C'_A(s)}{Q'(s)}$ and $\frac{T'(s)}{C'_{A0}(s)}$ Part 2

We can then substitute the original constants back into the transfer functions to get the final transfer functions. The transfer functions are shown below:

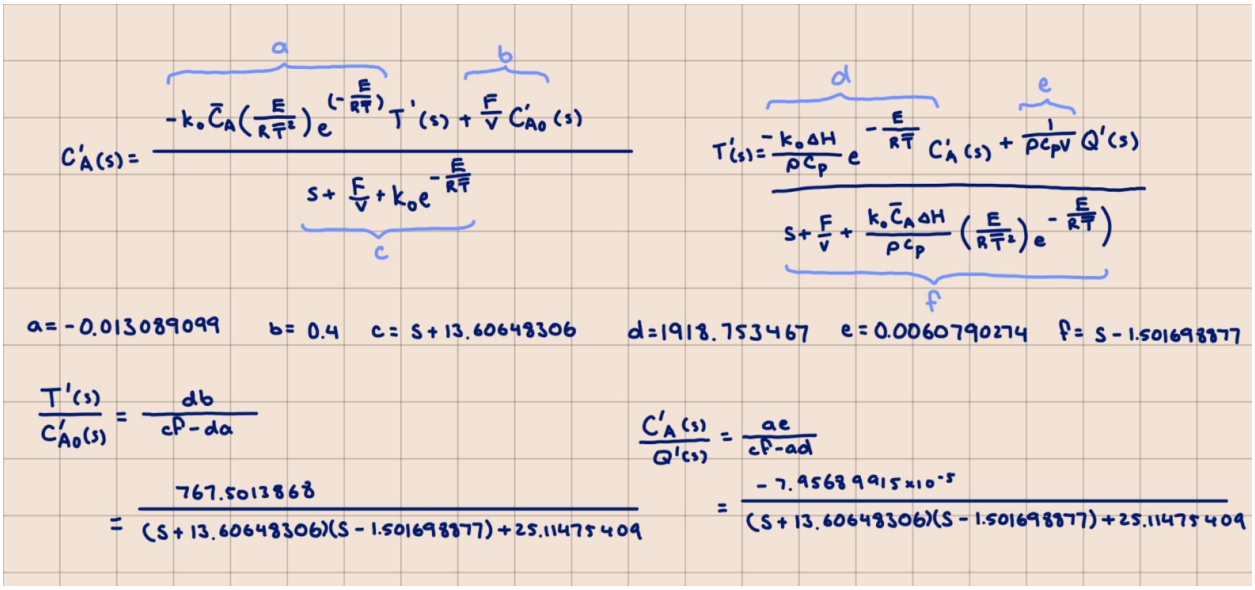

Figure 19: Final Transfer Functions $\frac{C'_A(s)}{Q'(s)}$ and $\frac{T'(s)}{C'_{A0}(s)}$

With these new transfer functions, we can relate the inputs C'_{A0} and Q' to the outputs C'_A and T' in the block diagram.

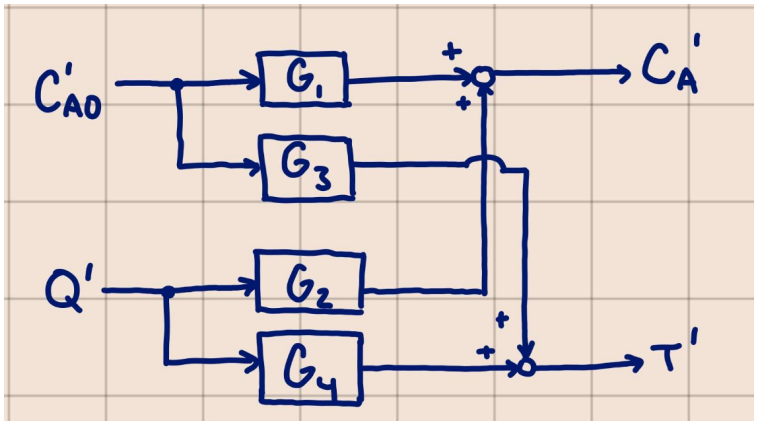

Figure 20: Block Diagrams Relating $C'_{A0}(s)$ and $Q'(s)$ to $C'_A(s)$ and $T'(s)$